

Quasi-Free Methyl Rotation in Zeolitic Imidazolate Framework-8

Wei Zhou,^{*,†,‡} Hui Wu,^{†,‡} Terrence J. Udovic,^{*,‡} John J. Rush,^{†,‡} and Taner Yildirim^{†,§}

NIST Center for Neutron Research, National Institute of Standards and Technology, 100 Bureau Dr., MS 6102, Gaithersburg, Maryland 20899, Department of Materials Science and Engineering, University of Maryland, College Park, Maryland 20742, and Department of Materials Science and Engineering, University of Pennsylvania, Philadelphia, Pennsylvania 19104

Received: August 6, 2008; Revised Manuscript Received: September 23, 2008

Using neutron inelastic scattering and diffraction, we have studied the quantum methyl rotation in zeolitic imidazolate framework-8 (ZIF-8: $\text{Zn}(\text{MeIM})_2$, MeIM = 2-methylimidazolate). The rotational potential for the CH_3 groups in ZIF-8 is shown to be primarily 3-fold in character. The ground-state tunneling transitions at 1.4 K of $334 \pm 1 \mu\text{eV}$ for CH_3 groups in hydrogenated ZIF-8 (H-ZIF-8) and $33 \pm 1 \mu\text{eV}$ for CD_3 groups in deuterated ZIF-8 (D-ZIF-8) indicate that the barrier to internal rotation is small compared to almost all methylated compounds in the solid state and that methyl–methyl coupling is negligible. A $2.7 \pm 0.1 \text{ meV}$ scattering peak assigned to the ground-state to first-excited-state, hindered rotational transition for H-ZIF-8, combined with a $\sim 3 \text{ meV}$ activation energy for methyl-group 3-fold jump reorientation estimated by quasi-elastic neutron scattering, suggests a very low methyl rotational barrier of $\sim 7 \text{ meV}$. Results are compared to the CH_3 rotational amplitude at 3.5 K derived from neutron diffraction data, which are also consistent with a small 3-fold barrier and a very low energy rotational oscillation.

I. Introduction

Zeolitic imidazolate frameworks (ZIFs)^{1,2} are a new class of framework compounds made up of MN_4 ($\text{M} = \text{Co}, \text{Cu}, \text{Zn}$, etc.) clusters linked together with imidazolate ligands to provide tunable nanosized pores and properties similar to those displayed by classical metal–organic frameworks. These materials also possess the chemical stability and structural diversity of zeolites and thus have the potential for many applications including hydrogen and methane storage.^{2,3} ZIF-8 ($\text{Zn}[\text{MeIM}]_2$, MeIM = 2-methylimidazolate) is the most well-known, prototypical ZIF compound, with a SOD (sodalite) zeolite-type structure. The unit cell of ZIF-8 is shown in part a of Figure 1.

One intriguing feature of the ZIF-8 structure is its methyl groups, which are bound to the imidazolate ligands (part b of Figure 1). Generally, the reorientational motion of the methyl group can be well described by classical random jumps at high temperature, whereas at low temperature it is dominated by quantum-mechanical rotational tunneling. Methyl-group dynamics in a large number of other molecular solids has been investigated since the 1970s.⁴ Several factors make ZIF-8 relatively unique. First, there exists only one type of methyl group in its structure, avoiding the complexity of mixed, multitype methyl-group dynamics. Second, the framework-bonded methyl group is oriented toward the large cavity of the porous ZIF-8 structure, and thus is expected to exhibit very rapid 1D rotation. Third, the distance between two neighboring methyl groups is large, making the methyl–methyl coupling weak. All of these features make ZIF-8 a prototype material for studying quasi-free methyl-group rotation.

In the work described here, we have studied the rotational dynamics and potential of the methyl groups by neutron

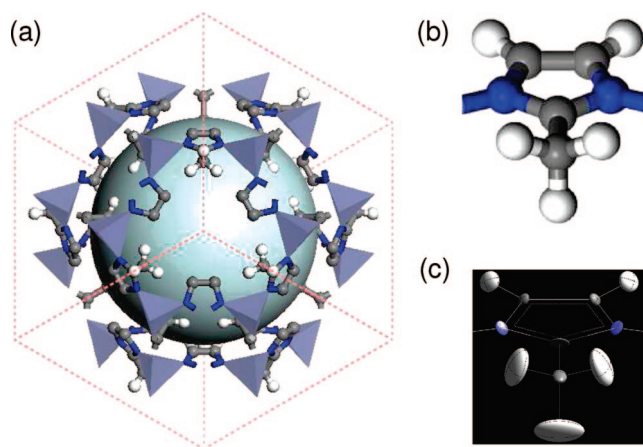


Figure 1. (a) Crystal structure of ZIF-8 ($I43m$). The 3D open framework consists of ZnN_4 clusters (the tetrahedra) connected by 2-methylimidazolate linkers. The large sphere at the center denotes the pore structure of ZIF-8. For clarity, some H atoms on the linkers (except those belonging to the methyl groups) are not shown. (b) The structure of the 2-methylimidazolate linker. (c) The ellipsoids of the MeIM linker obtained from neutron diffraction data from H-ZIF-8 at 3.5 K. The methyl groups bound to the imidazolate ligand exhibit very large torsional amplitudes, even at very low temperature, suggesting a low barrier to 1D rotation.

spectroscopy and diffraction including measurements on both fully hydrogenated (H-ZIF-8) and fully deuterated (D-ZIF-8) compounds.

II. Materials and Methods

H-ZIF-8 was synthesized using a solvothermal method as described in ref 2. D-ZIF-8 was synthesized using a deuterated 2-methylimidazolate precursor. All measurements were made at the National Institute of Standards and Technology Center for Neutron Research. Neutron powder diffraction (NPD) data

* To whom correspondence should be addressed. Email: wzhou@nist.gov (W. Z.), udovic@nist.gov (T. J. U.).

[†] National Institute of Standards and Technology.

[‡] University of Maryland.

[§] University of Pennsylvania.

were collected on the High-Resolution Neutron Powder Diffractometer (BT-1).⁵ Neutron spectroscopy data were collected using the Fermi-Chopper Spectrometer (FCS),⁶ Disk-Chopper Spectrometer (DCS),^{6,7} and High Flux Backscattering Spectrometer (HFBS).⁸ The three instruments cover different energy ranges and provide different energy resolutions. Rietveld refinements on the NPD patterns were performed using the GSAS package⁹ without any imposed constraints or soft restraints.

III. Results and Discussion

A. Methyl-Group Structure. As mentioned earlier, all MeIM linkers in the ZIF-8 structure are crystallographically equivalent. Several of us have recently published a neutron diffraction study of the structure of ZIF-8.³ To obtain more detailed structural information on the methyl group, we measured the NPD pattern of both the H-ZIF-8 and the D-ZIF-8 samples in the temperature range of 3.5–300 K. For both samples, the host lattice maintains the same crystalline phase over the whole temperature range, with lattice parameters slightly increasing with increasing temperature. Structural refinements with anisotropic thermal factors gave excellent data fits. Details of the crystallographic parameters derived from our structure refinements for ZIF-8 between 3.5 and 200 K are shown in the Supporting Information for this article. In Figure 2, we show the NPD data from D-ZIF-8 measured at 3.5 and 200 K along with the Rietveld structure refinements. From the 3.5 K data, the average C–D bond lengths for C–D2A and C–D2B (where D2A and D2B are the two crystallographically distinct methyl-group D atoms) are 1.01 and 0.94 Å, respectively. The D2A–C–D2A and D2A–C–D2B bond angles are 103.0 and 105.8°, respectively. The parameters of H-ZIF-8 are similar. Thus, the deviation from the fully 3-fold symmetric configuration of the methyl groups is small.

The thermal ellipsoids for atoms in the MeIM linker from the hydrogenated sample at 3.5 K are shown in part c of Figure 1 as an example. It should be noted that the torsional amplitudes are quite large but suggest a mainly 3-fold character for the rotational potential. The mean-square amplitudes θ^2 (in radians²) for the rotational motion of the methyl groups can be derived for D(H)2A and D(H)2B using the thermal parameters. The torsional energies E were then estimated using the expression relating energies to mean-square amplitudes of motion for a harmonic oscillator¹⁰ (although the “harmonic assumption” is clearly questionable for such a large rotational amplitude):

$$\theta^2 = \frac{B}{E} \coth\left(\frac{E}{2kT}\right) \quad (1)$$

where the rotational constant $B = \hbar^2/(2I)$ and I is the CH₃ or CD₃ moment of inertia. Therefore, with the average values of θ^2 for D(H)2A and D(H)2B and the equation above, we estimated average energies for the CH₃ and CD₃ oscillations. The methyl groups exhibit large rotational amplitudes, corresponding to torsional energies of ~ 2.9 meV for CH₃ and ~ 1.7 meV for CD₃ at 3.5 K, which are consistent with a very low rotational barrier. At higher temperatures, these amplitudes tend toward a more uniform proton density around the 3-fold methyl-group axis.

The open structure of the framework indeed implies a low barrier for the methyl-group rotation in this structure. The minimum C–C distance between the adjacent methyl groups is 4.35 Å and the smallest intermolecular H–H distance is 2.84 Å. This large distance between nearest-neighbor methyl groups further suggests that the coupling between methyl groups is very small.

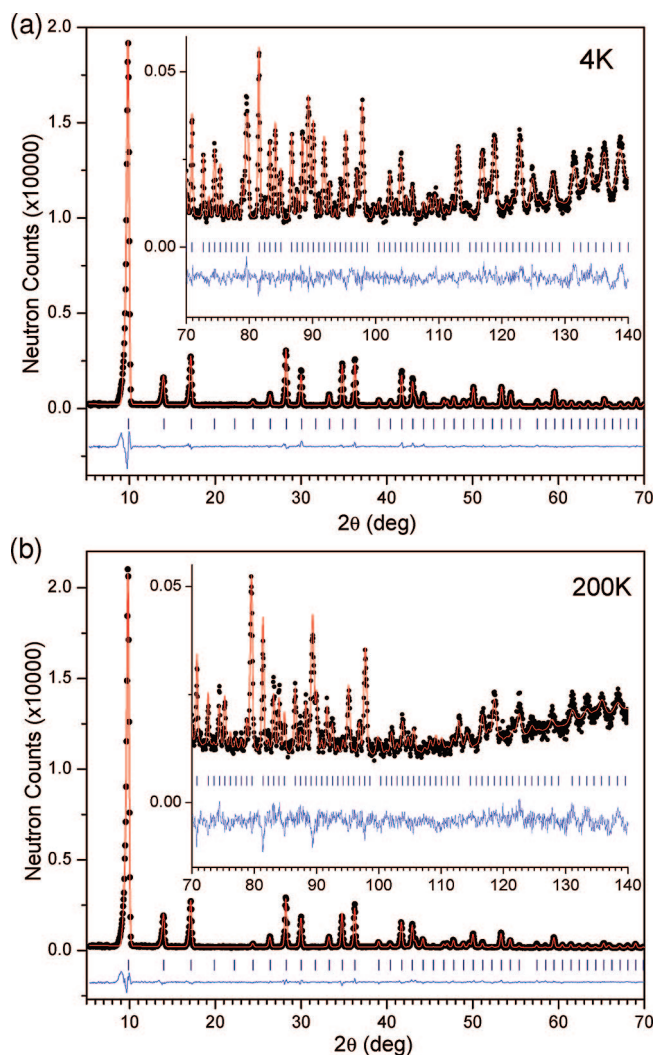


Figure 2. Observed (dots), refined (line), and difference (noisy line) neutron powder diffraction profiles ($\lambda = 2.079$ Å) for deuterated ZIF-8 measured at (a) 3.5 K and (b) 200 K.

B. Methyl-Group Tunneling and Rotation. For a 1D rigid rotation, it is well established that the quantum rotational levels are determined by the solutions E_i of the stationary Schrödinger equation:

$$H\Psi_i = E_i\Psi_i \quad (2)$$

with the Hamiltonian:

$$H = -B\frac{\partial^2}{\partial\phi^2} + V(\phi) \quad (3)$$

where $V(\phi)$ is the rotational potential. The rotational constant B of CH₃ is ~ 0.655 meV. The solution of the Schrödinger equation can be carried out numerically.¹¹ For a free CH₃ rotor, $V(\phi) = 0$, and the $J = 0 \rightarrow 1$ transition energy (splitting of the ground-state rotational level) is equal to B . For a nonzero rotational barrier, this energy decreases with increasing barrier height.

To quantitatively probe the methyl-group rotations, we have directly measured the $0 \rightarrow 1$ rotational transition using neutron spectroscopy. The results for H-ZIF-8 using DCS with 7 Å neutrons (~ 18 μ eV resolution) are shown in Figure 3. The observed $0 \rightarrow 1$ rotational peak at 334 ± 1 μ eV, which we refer to as a tunneling peak, again implies a very low rotational barrier. Note that the peak is rather sharp and there is no obvious

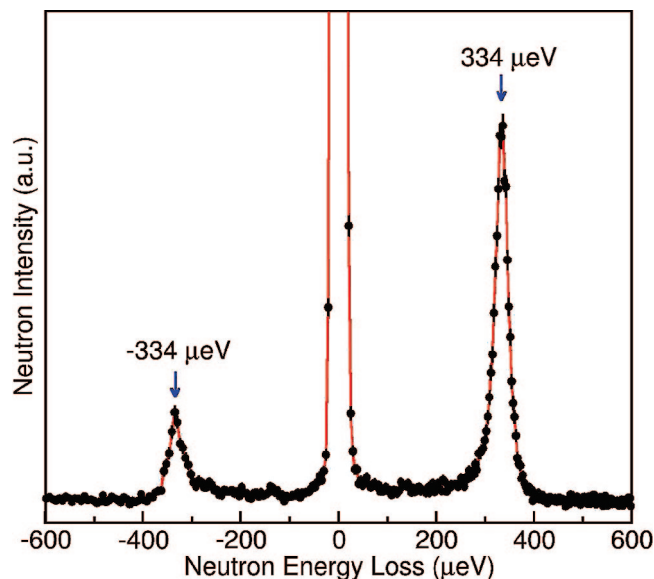


Figure 3. Tunneling spectrum of H-ZIF-8 at 1.4 K using DCS with 7 Å neutrons. Vertical error bars denote $\pm 1\sigma$. The relatively high energies [at $\pm 334 \pm 1 \mu\text{eV}$] imply a low rotational barrier. Also note that there are no obvious split modes, suggesting very small methyl–methyl coupling.

mode splitting, again indicating negligible methyl–methyl coupling. Also note that the tunneling peak is not perfectly symmetrical, with a small tail on the low-energy side, which could be due to a small deviation of the methyl-group potential from perfect 3-fold symmetry.

To further probe the nature of the rotational potential, we have measured the tunneling spectrum of D-ZIF-8 using both HFBS ($\sim 1 \mu\text{eV}$ resolution) and DCS (9 Å neutrons, $18 \mu\text{eV}$ resolution). From the results of both measurements (Figure 4), we locate a peak at $33 \pm 1 \mu\text{eV}$, which is assigned to the CD_3 tunneling transitions (at much lower energy due to the twice as large CD_3 moment of inertia compared to CH_3). We have extended the DCS measurements to search for higher rotational levels using 3.6 and 4 Å neutrons (i.e., 6.3 and 5.1 meV incident energies, respectively). The results (Figure 5) show a broad peak at $2.7 \pm 0.1 \text{ meV}$ (based on the higher-resolution 4 Å data), which we tentatively assign to the second rotational level for H-ZIF-8, although the higher-resolution H-ZIF-8 spectrum suggests that framework modes could also be contributing and/or overlapping here, causing some uncertainty in the peak position. Nonetheless, this peak is generally consistent with the $\sim 2.9 \text{ meV}$ hindered rotational energy derived above from the diffraction mean-square amplitudes. No analogous mode was observed for D-ZIF-8 in Figure 5, due to much weaker scattering from the deuterated methyl groups. Both H-ZIF-8 and D-ZIF-8 spectra show evidence of a weaker maximum near 1.2 meV, which we ascribe to a low-energy framework mode. If we assume a 3-fold barrier to rotation, the $334 \mu\text{eV}$ tunnel splitting for H-ZIF-8, combined with a second rotational level of 2.7 meV, predicts a barrier height of 6 meV. For comparison, the $33 \mu\text{eV}$ tunnel splitting for D-ZIF-8 suggests a barrier of about 8 meV for the CD_3 groups, again assuming 3-fold character.

We have also studied the evolution of the tunneling peaks versus temperature. Figure 6 displays FCS measurements for H-ZIF-8 using 6 Å neutrons ($\sim 70 \mu\text{eV}$ resolution), which show that, at higher temperatures (30 K and above), the methyl tunneling peaks disappear and transform into a quasi-

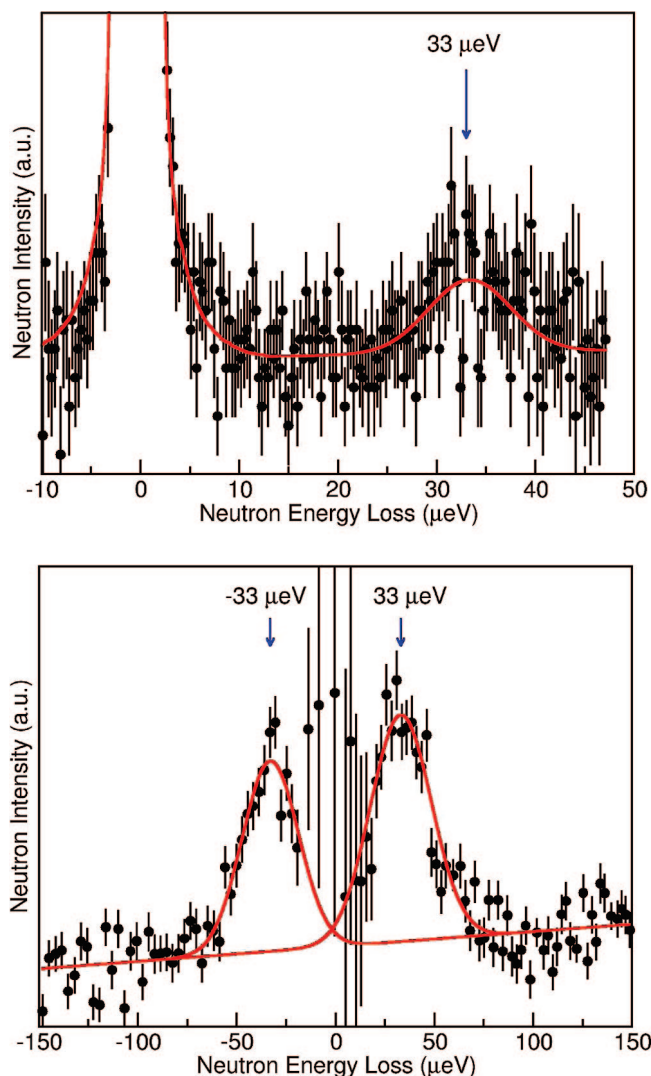


Figure 4. Tunneling spectra of D-ZIF-8 at 1.4 K using (top) HFBS [with a tunneling peak at $33 \pm 1 \mu\text{eV}$] and (bottom) DCS with 9 Å neutrons. Vertical error bars denote $\pm 1\sigma$. The DCS spectrum shown is actually a difference spectrum; i.e., to enhance the DCS tunneling peaks [at $\pm 33 \pm 2 \mu\text{eV}$], the low-temperature elastic scattering was largely removed by subtracting a 30 K spectrum (scaled $1.04\times$) from the 1.4 K spectrum.

elastic peak that broadens with increasing temperature. Thus, by coupling to lattice phonons, the low-temperature coherent quantum rotation (tunneling) changes into a classical stochastic jump reorientation (hopping) as the ground-state tunneling peaks shift toward the elastic line and broaden.

These results also provide information on the rotational dynamics at low temperature in ZIF-8, and an examination of the quasi-elastic peaks from H-ZIF-8 gives another clear indication of a very low barrier. Figure 7 shows the temperature dependence of the full width at half-maximum (fwhm) quasi-elastic linewidths (Γ) for H-ZIF-8 obtained from DCS measurements using 5 Å neutrons ($\sim 90 \mu\text{eV}$ resolution), plotted in an Arrhenius fashion [$\ln(\Gamma)$ vs. T^{-1}]. The activation energy E_a for 3-fold jump reorientation can be estimated from the slope E_a/k , where k is Boltzmann's constant. We would point out that E_a is derived under the assumption that the methyl groups reorient through a jump diffusion process by thermal activation over the barrier (~ 6 – 8 meV). At the higher temperatures in this study (> 40 – 50 K), this model loses its validity as the thermal energy is comparable to the barrier height. The transformation from

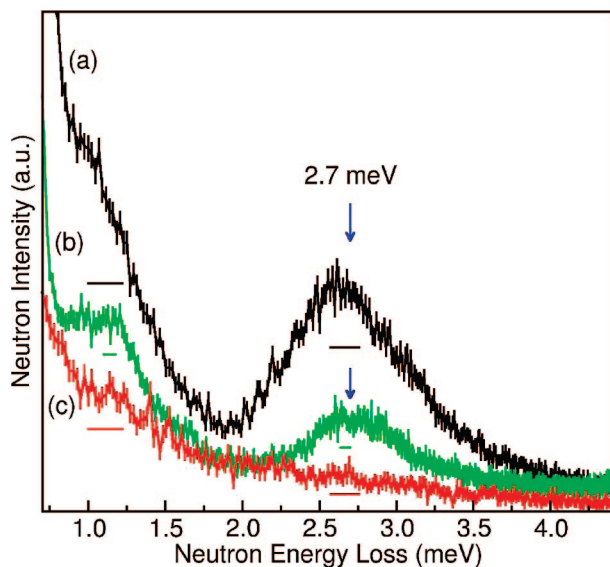


Figure 5. DCS spectra (1.4 K) measured for H-ZIF-8 with (a) 3.6 Å neutrons and (b) 4 Å neutrons, and (c) for D-ZIF-8 with 3.6 Å neutrons. Instrumental resolution is denoted by the horizontal bars. Vertical error bars denote $\pm 1\sigma$.

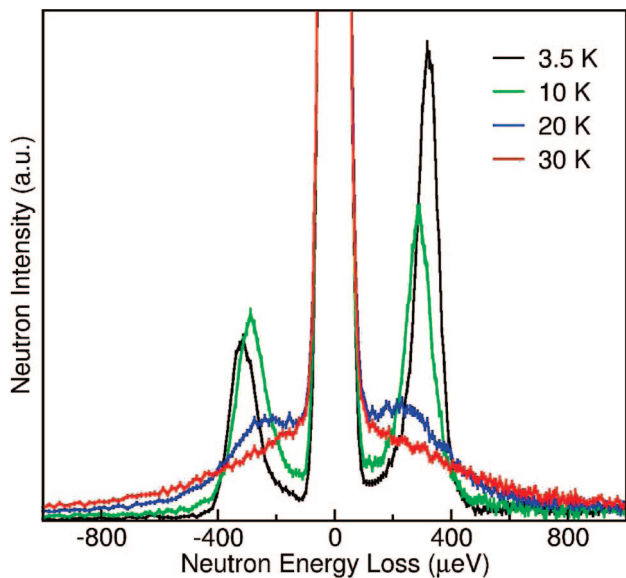


Figure 6. Temperature evolution of the tunneling spectrum of H-ZIF-8 using FCS with 6 Å neutrons. Vertical error bars denote $\pm 1\sigma$. At higher temperature, classical jump reorientation leads to quasi-elastic scattering.

3-fold jump diffusion to rotational diffusion is manifested by the nonlinear nature of the Arrhenius plot with increasing temperature. We estimate an E_a of ~ 3 meV from the data between 30 and 40 K, assuming that we are largely in the jump-diffusion regime in this low-temperature region. Further assuming that the E_a determined at these temperatures is a measure of the distance from the first-excited rotational ($J = 2$) level (tentatively assigned at 2.7 meV above the ground-state level) to the top of the rotational-potential barrier and estimating a zero-point energy of $1/2(2.7 \text{ meV})$ leads to a barrier height of ~ 7 meV, which is close to that predicted above for a pure 3-fold potential. The DCS results at 1.4 K with 4 Å neutrons have also been analyzed to obtain an elastic incoherent structure factor (EISF) for the methyl-group hydrogens versus momentum transfer Q (Figure 8). The Q dependence of the EISF is

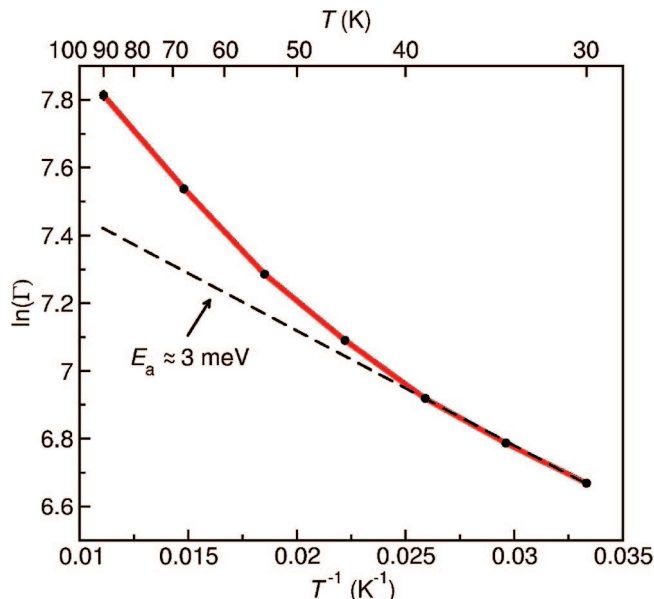


Figure 7. Plot of $\ln(\Gamma)$ vs T^{-1} for H-ZIF-8 between 30 and 90 K, where Γ (in μeV) is the fwhm quasi-elastic line width, obtained using DCS with 5 Å neutrons. Experimental uncertainties are commensurate with symbol size.

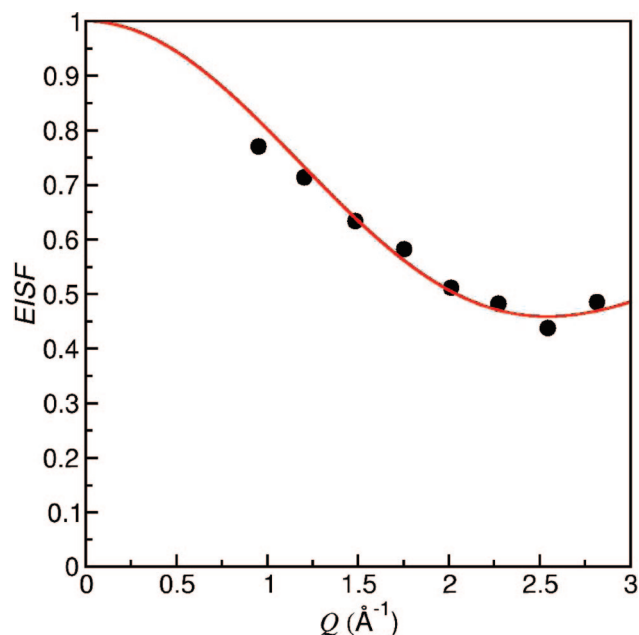


Figure 8. EISF for H-ZIF-8 from 1.4 K DCS data with 4 Å neutrons, fit with the model curve for 3-fold rotational tunneling.¹¹ Experimental uncertainties are commensurate with symbol size. The resulting hydrogen-tunneling radius is $1.04 \pm 0.01 \text{ Å}$.

consistent with the model curve for 3-fold rotational tunneling.¹¹

$$\text{EISF} = \frac{5 + 4j_0(Qr\sqrt{3})}{9} \quad (4)$$

where j_0 is the zeroth-order spherical Bessel function and r is the hydrogen tunneling radius. From the model fit, we obtained a tunneling radius of $1.04 \pm 0.01 \text{ Å}$, which is close to the value determined by NPD. More details are found in the Supporting Information.

IV. Concluding Remarks

All of the results of our extensive study show the existence of an unusual quasi-free rotational potential for CH_3 groups in

ZIF-8 when compared to most other methylated compounds⁴ in the solid state. The high methyl-group tunneling energies and low hindered rotational transitions, combined with the results of quasi-elastic neutron scattering between 30 and 40 K, provide a largely 3-fold rotational barrier of about 7 meV. Two previous examples of quasi-free methyl rotation are 4-methyl pyridine^{12–14} and lithium acetate dihydrate,¹⁵ which have high tunneling energies and thus presumably low rotational barriers. Yet, both molecular solids show methyl–methyl coupling effects, which result in complex tunneling spectra. In contrast, the spectrum of ZIF-8 shows no evidence of sidebands, which indicates independent rotation of CH₃ groups.

Recently, several of us have determined the structural arrangement of hydrogen and methane molecules adsorbed in ZIF-8 through neutron diffraction.^{3,16} It is also of interest to study the effects of the adsorption of such gases on the methyl-group rotational potential and dynamics in ZIF-8. These effects should be considerable due to the ease of perturbing the potential experienced by the quasi-free rotating methyl groups. Such a study is underway, and the results will be presented in a future article.

Acknowledgment. The authors thank C. M. Brown for technical help in the DCS data collection and G. Gasparovic for assistance in the HFBS data collection. This work utilized facilities supported in part by the National Science Foundation under Agreement No. DMR-0454672. We also acknowledge partial DOE support from EERE Grant No. DE-AI-01-05EE11104 and BES Grant No. DE-FG02-08ER46522.

Supporting Information Available: Details associated with the determination of quasi-elastic linewidths and low-temper-

ature elastic incoherent structure factors. Crystallographic parameters derived from structure refinements for ZIF-8 between 3.5 and 200 K. This material is available free of charge via the Internet at <http://pubs.acs.org>.

References and Notes

- (1) Huang, X. C.; Lin, Y. Y.; Zhang, J.-P.; Chen, X. M. *Angew. Chem., Int. Ed.* **2006**, *45*, 1557–1559.
- (2) Park, K. S.; Ni, Z.; Cote, A. P.; Choi, J. Y.; Huang, R.; Romo, F. J.; Chae, H. K.; O'Keefe, M.; Yaghi, O. M. *Proc. Natl. Acad. Sci. U.S.A.* **2006**, *103*, 10186.
- (3) (a) Wu, H.; Zhou, W.; Yildirim, T. *J. Am. Chem. Soc.* **2007**, *129*, 5314–5315. (b) Zhou, W.; Wu, H.; Hartman, M. R.; Yildirim, T. *J. Phys. Chem. C* **2007**, *111*, 16131–16137.
- (4) Prager, M.; Heidemann, A. *Chem. Rev.* **1997**, *97*, 2933.
- (5) <http://www.ncnr.nist.gov/instruments/bt1/>.
- (6) Copley, J. R. D.; Udovic, T. J. *J. Res. NIST* **1993**, *98*, 71–87.
- (7) Copley, J. R. D.; Cook, J. C. *Chem. Phys.* **2003**, *292*, 477–485.
- (8) <http://www.ncnr.nist.gov/instruments/hfbs/>.
- (9) Larson, A. C.; Von Dreele, R. B. *General Structure Analysis System*; Report LAUR 86–748; Los Alamos National Laboratory: New Mexico, 1994.
- (10) Prince, E.; Schroeder, L. W.; Rush, J. J. *Acta. Crystallogr. B* **1973**, *29*, 184.
- (11) Press, W. *Single Particle Rotations in Molecular Crystals*; Springer Tracts in Modern Physics; Springer: Berlin, 1981; Vol. 92.
- (12) Fillaux, F.; Carlile, C. J. *Phys. Rev. B* **1990**, *42*, 5990–6006.
- (13) Fillaux, F.; Carlile, C. J.; Kearley, G. J. *Phys. Rev. B* **1991**, *44*, 12280–12293.
- (14) Fillaux, F.; Carlile, C. J.; Kearley, G. J. *Phys. Rev. B* **1998**, *58*, 11416–11419.
- (15) Nicolai, B.; Cousson, A.; Fillaux, F. *Chem. Phys.* **2003**, *290*, 101–120.
- (16) Wu, H.; Zhou, W.; Yildirim, T. (private communication).

JP807033M